ISBN: 978-3-95450-247-9 ISSN: 2673-5490 doi: 10.18429/JACoW-IPAC2024-THPS26

CRYOGENIC PERMANENT MAGNET UNDULATOR AT HIGH BEAM CURRENTS*

J.-C. Huang†, C.-S. Yang, P.-S. Chuang, C.-L. Chen, National Synchrotron Radiation Research Center, HsinChu, Taiwan
H. Kitamura , RIKEN SPring-8 Center, Hyogo, Japan

© Content from this work may be used under the terms of the CC BY 4.0 licence (© 2024). Any distribution of this work must maintain attribution to the author(s), title of the work, publisher, and DOI.

Abstract

Cryogenic permanent-magnet undulators (CPMUs) have become a point of interest in the development of short-period undulators. However, electron beam-induced heating presents a significant challenge to CPMU development. The CU15, the first CPMU at NSRRC, demonstrates exceptional spectral and operational performance, even when operating at small gaps with a beam current of 500 mA over three years.

INTROUDCTION

Cryogenic permanent magnet undulators are widely regarded as a highly promising option for the development of short-period undulators aimed at improving the brilliance of synchrotron radiation. The technologies related to TPS-CPMU (CU15) have been well-documented [1,2]. However, using small-gap CPMUs in storage rings poses several challenges, such as beam lifetime, injection aperture, demagnetization from radiation, beam-induced heating, and safety concerns. One of the challenges at the TPS storage ring is beam-induced heating because the storage ring currently operates at a beam current of 500 mA with a short bunch length (~17 ps), which intensifies the beam-induced heating on CPMU components. This report focuses on the beam-induced heating issue.

COMMISIOING OF CU15

In 2019, CU15 was first installed in the storage ring for test runs. The transition taper prototype (Fig. 1(A)) was made of 0.2 mm thick Be-Cu sheets [2][3] to accommodate the opening and closing of the magnet gap and temperature variations in the magnet array length.

During the first week, CU15 could be operated with a beam current of 300 mA under the condition that the magnet temperature was kept at 80 K. As the beam current gradually increased to 500 mA, the cooling capacity of the cryo-cooler could no longer suppress the temperature rise due to the beam. As the beam current gradually increased to 500 mA, the cooling capacity of the cryocooler was no longer sufficient to suppress the temperature rise due to the beam, and the equilibrium temperatures of the magnet and the prototype taper reached 256 K and 410 K, respectively.

After an exhaustive investigation, it was found that the problem is attributed to the transition tapers at both ends of the CU15. The high beam-induced heating appears to be due to the cavity-like shape of the transition tapers. In other words, the high deformability of the elongated beryllium copper (BeCu) sheet caused the formation of a cavity-like structure (see Fig. 1(B)). The photo in Fig. 1(B) was taken at room temperature, but the above shape remains to a certain extent even when the CPMU is operated at 80K. Therefore, these cavity-like structures must be causing beam energy loss and generating beam-induced heating of up to several hundred watts.

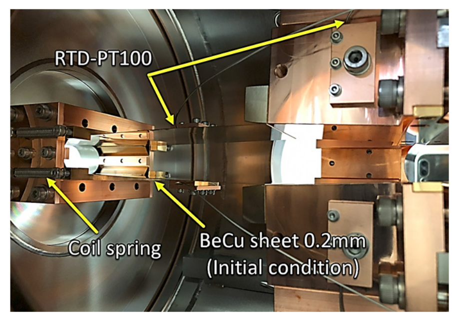

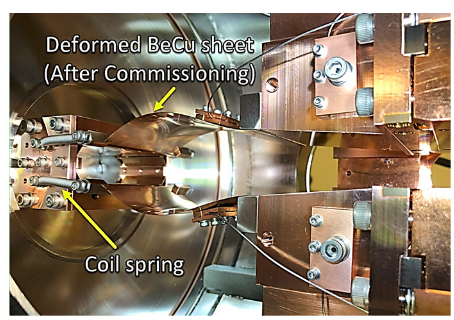

Figure 1: (A) (upper figure) Prototype transition tapers installed in CU15; (B) (lower figure) Transition tapers deformed after beam-heating.

As shown in Fig. 2, an improved transition taper with a water-cooled section in the middle was developed to solve the problems of the prototype transition taper. In this improved transition taper, microwave power trapping is minimized by adopting a straight taper structure. The water cooling system efficiently absorbs most of the heat generated at the taper, reducing the load on the cryocooler. Furthermore, the use of a double-layered sheet of 0.15 mm thick stainless steel with 0.01 mm thick copper plating not only minimizes the heat generated by the image current, but also provides high insulation for the magnet array.

The beam-induced heating shown in Fig. 3 exhibits a strong quadratic-dependent correlation to the beam current,

* Work supported by National Science and Technology Council, Taiwan
† huang.juiche@nsrrc.org.tw

ISBN: 978-3-95450-247-9 ISSN: 2673-5490 doi: 10.18429/JACoW-IPAC2024-THPS26

indicating that the heating source is due to a broadband impedance. The heat load generated by the prototype transition taper is about twice that of the modified taper, and the cooling capacity is insufficient when the beam current exceeds 350 mA. Figure 3 also shows that the improved prototype transition taper without a cavity-like structure reduced the beam heating of the CPMU to less than 100 W.

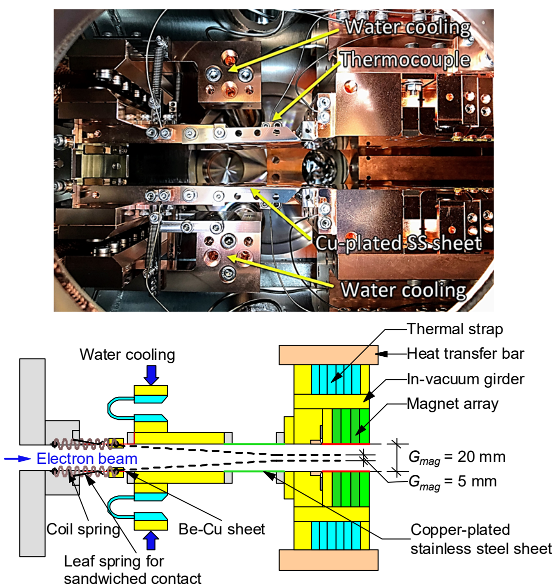

Figure 2: (A) (upper figure) A modified transition taper (B) (lower figure) the configurations of modified transition taper to facilitate the CPMU operation at a beam current of 500 mA.

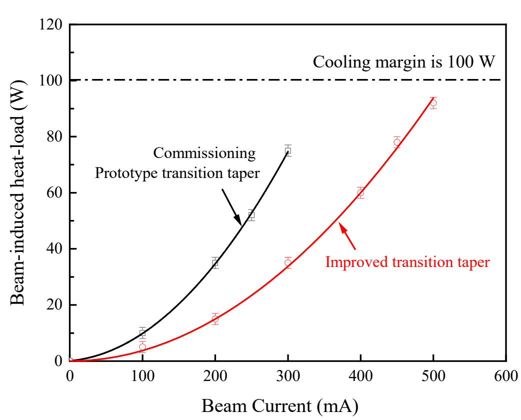

Figure 3: Beam-induced heat-load varies with beam current with magnet gap of 20 mm and temperature of magnets at 80 K. The solid lines represent quadratic curve fitting. RF voltage is 3.2MW.

BEAM-INDUCED HEATING

The beam-induced heating mechanism is examined and explained in reference [2]. The heating mechanism originates when the electron beam passes through a non-zero impedance section, such as tapers, losing some of its energy due to geometric impedance. Part of the energy loss appears as microwaves, either trapped in the taper or magnet section, or propagating along the electron orbit. Furthermore, external microwave power generated from the geometric impedance of various components located upstream or downstream of CU15 (such as the BPM, bellows, and other vacuum components) also propagates and is trapped within the taper section, causing an increase in the temperature of the transition tapers or end of magnet arrays. The primary heat-load on magnet arrays of TPS-CPMU is derived from the internal and external microwave power due to geometric impedance.

The temperature distribution across the magnet arrays is shown in Fig. 4. The temperature distribution profile is symmetrical and parabolic at the center of the magnet array, with temperature rises observed near both ends. This suggests that the contribution of SR irradiation is very small. Therefore, the temperature increases near both ends seem to be primarily due to microwaves propagating into the magnet gap from both ends of the magnet array. The temperature increases near both ends become more pronounced when the magnet gap is narrower, and the bunch lengths are shorter. This phenomenon can be explained by the microwaves passing through the magnet gap and being absorbed by the magnet array. A wider magnet gap may allow for a longer distance of microwave propagation, whereas a narrow gap may result in a shorter propagation distance. Consequently, when the magnet gap is narrow, temperatures near the ends of the magnet arrays are thought to be higher compared to the center.

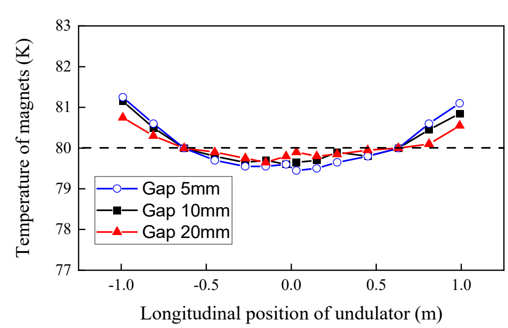

Figure 4: Temperature distribution across magnet arrays at gaps of 5, 10 and 20 mm, with a beam current of 500 mA.

The observation of temperature rise occurs not only at the end of the magnet arrays but also at the end flange of CU15 (Fig. 5a). The temperature of the flange reaches around 56 °C at 500 mA. Local overheating has been measured by the thermal infrared (IR) camera (Fig. 5b,5c) and Resistance Temperature Detector (RTD) sensors. The heating power is estimated to be more than 20 W from separate experiments, significantly higher than the value estimated from the geometric impedance of the flanges.

Figure 6 shows the dependence of the downstream and upstream temperature rise on the beam current. As shown in Fig. 6, the increased temperature follows a quadratic correlation with beam current, suggesting that the heating

Content from this work may be used under the terms of the CC BY 4.0 licence (© 2024). Any distribution of this work must maintain attribution to the author(s), title of the work, publisher, and DOI.

ISBN: 978-3-95450-247-9 ISSN: 2673-5490 doi: 10.18429/JACoW-IPAC2024-THPS26

© Content from this work may be used under the terms of the CC BY 4.0 licence (© 2024). Any distribution of this work must maintain attribution to the author(s), title of the work, publisher, and DOI.

source is from broadband impedance (geometric impedance). The power heating the flanges is considered to be derived from the sum of external and internal microwave.

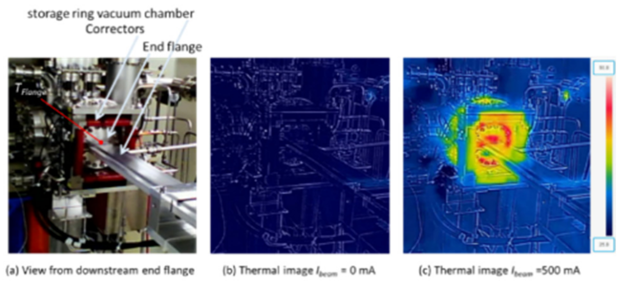

Figure 5: Thermal image from downstream vacuum chamber of CU15 by thermos IMAGER TIM40.

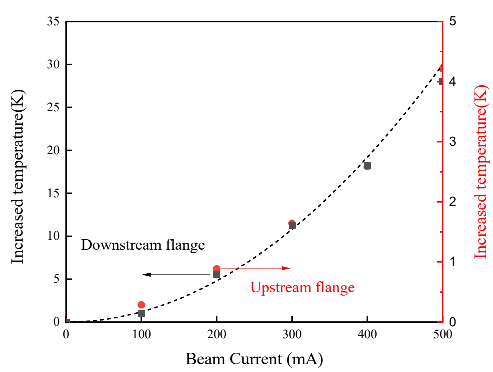

Figure 6: Temperature increased at upper and low flanges, measured by RTD.

PHOTON FLUX

Figure 7 shows the flux density from two undulators (IU22-3m, period length of 15 mm and a period number of 142 ; CU15-2m, period length of 15 mm and a period number of 133) in different harmonics. The calculated spectral performance of CU15-2m is superior to that of IU22-3m at energy around 15 keV.

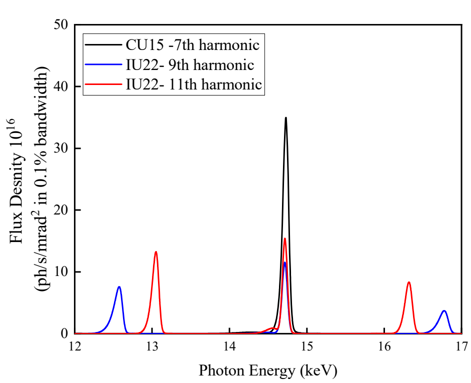

Figure 7: Flux Density calculated from IU22 and CU15, using SPECTRA [4].

To validate this result, a comparison was conducted in the powder diffraction beamline. The same MYTHEN detector was used to measure photon counts from an identical diffraction peak of a NIST standard material 660c (LaB6) using CU15 and IU22. The results presented in Table 1 demonstrates that CU15 can generate a photon flux, exhibiting a maximum increase three times higher than that of IU22. This result aligns well with the spectral calculations. Feedback from users in the experimentation also confirms that by replacing IU22-3m with CU15-2m, the measurement time reduced to one-third of the original duration.

Table 1: Measured Photon Counts of Sample between CU15-2m and IU22-3m

	Harmonics @~ 15 keV	Gap (mm)	Relative photon counts*
CU15-2m	7th	5.075	4.6
IU22-3m	9th	8.010	1.1
	11th	6.530	1.4

*Normalized in 1mA beam current × 10^3

SUMMARY

The CU15-2m has successfully operated in the TPS storage ring at NSRRC with a beam current of 500 mA for more than three years. The primary heat-load on magnet arrays is generated by the microwave power caused by beam energy loss due to geometric impedance. The photon flux has been verified by the powder diffraction beamlines, showing that CU15-2m is superior to IU22-3m.

Conduction-cooled CPMU is now poised for commercial production based on these successful experiences. In general, the CPMU is feasible for operation at a small gap in most 4th generation storage rings, provided the bunch length is sufficiently long.

REFERENCES

[1] J. C. Huang *et al.*, "Challenges of in-vacuum and cryogenic permanent magnet undulator technologies", *Phys. Rev. Accel. Beams*, vol. 20, p. 064801, June 2017. doi: 10.1103/PhysRevAccelBeams.20.064801

[2] J. C. Huang et al., "Performance of TPS Cryogenic Permanent Magnet Undulators at NSRRC", in *Proc. 10th Int. Particle Accelerator Conf. (IPAC'19)*, Melbourne, Australia, May 2019, pp. 4278-4289. doi:10.18429/JACoW-IPAC2019-THPTS071

[3] J. C. Huang *et al.*, "Performance investigation of conduction-cooled cryogenic permanent magnet undulator at high beam currents", *Phys. Rev. Accel. Beams*, vol. 27, p. 023501, Feb. 2024. doi: 10.1103/PhysRevAccelBeams.27.023501

[4] J. C. Huang *et al.*, T. Tanaka and H. Kitamura, "SPECTRA: a synchrotron radiation calculation code", *J. Synchrotron Rad.* vol. 8, p.1221, 2001. doi:10.1107/S090904950101425X